


Article

Adsorption Characteristics of Gas Molecules (H₂O, CO₂, CO, CH₄, and H₂) on CaO-Based Catalysts during Biomass Thermal Conversion with in Situ CO₂ Capture

Baofeng Zhao ^{1,*} , Jingwei Wang ¹, Di Zhu ¹, Ge Song ^{1,2}, Huajian Yang ¹, Lei Chen ¹, Laizhi Sun ¹, Shuangxia Yang ¹, Haibin Guan ¹ and Xinping Xie ¹

¹ Key Laboratory for Biomass Gasification Technology of Shandong Province, Energy Research Institute, Qilu University of Technology (Shandong Academy of Sciences), Jinan 250014, China

² School of Civil Engineering, University of Science and Technology Liaoning, Anshan 114051, China

* Correspondence: zhaobf@sderi.cn; Tel.: +86-0531-8260-5584

Received: 7 August 2019; Accepted: 2 September 2019; Published: 9 September 2019



Abstract: Biomass thermochemical conversion with in situ CO₂ capture is a promising technology in the production of high-quality gas. The adsorption competition mechanism of gas molecules (H₂O, CO₂, CO, CH₄, and H₂) on CaO-based catalyst surfaces was studied using density functional theory (DFT) and experimental methods. The adsorption characteristics of CO₂ on CaO and 10 wt % Ni/CaO (100) surfaces were investigated in a temperature range of 550–700 °C. The adsorption energies were increased and then weakened, reaching their maximum at 650 °C. The simulation results were verified by CO₂ temperature-programmed desorption (CO₂-TPD) experiments. By the density of states and Mulliken population analysis, CaO doped with Ni caused a change in the electronic structure of the O_{surf} atom and decreased the C–O bond stability. The molecular competition mechanism on the CaO-based catalyst surface was identified by DFT simulation. As a result, the adsorption energies decreased in the following order: H₂O > CO₂ > CO > CH₄ > H₂. The increase of CO₂ adsorption energy on the 10 wt % Ni/CaO surface, compared with the CaO surface, was the largest among those of the studied molecules, and its value increased from 1.45 eV to 1.81 eV. Therefore, the 10 wt % Ni/CaO catalyst is conducive to in situ CO₂ capture in biomass pyrolysis.

Keywords: in situ CO₂ capture; DFT; 10 wt % Ni/CaO; adsorption; CO₂-TPD

1. Introduction

Biomass thermochemical conversion with in situ CO₂ capture technology is one of the hotspots in biomass energy utilization research, which can produce high-quality fuel gas with a wide range of applications (alcohol/ether fuel synthesis, hydrogen fuel cells, etc.) [1–5]. The in situ CO₂ capture is the core process for the research and development of this technology because it can effectively remove CO₂, adjust the gas composition, and improve the quality of pyrolysis gas [6–10]. In order to enhance CO₂ adsorption capacity, CaO-based catalysts have been studied in biomass thermochemical conversion with in situ CO₂ capture [1–3,11–16]. Naeem et al. [11] utilized the Pechini method to synthesize Al₂O₃-, MgO-, Y₂O₃-stabilized, and CaO-based CO₂ sorbents. The experimental results exhibited high CO₂ uptake with improved cyclic stability and superior performance when compared to the performance of limestone-derived benchmark sorbent. Charisiou et al. [12] investigated the catalytic performance of H₂ production through the glycerol steam reforming reaction (GSR) of nickel catalysts supported on CaO–MgO–Al₂O₃. It was proved that the presence of CaO–MgO modifiers had an important effect on gaseous product distribution, leading to increased conversion to gaseous products.

In our previous studies [1–3], a Ni/CaO catalyst was developed in biomass pyrolysis for high-quality gas, which had a profound impact on the CO₂ adsorption capacity and catalytic cracking of tar effect at about 700 °C. However, at present, there are few researches on the mechanism of adsorption of CaO-based catalysts during biomass thermal conversion with in situ CO₂ capture.

The adsorption characteristics of CaO-based catalysts are impacted by multiple reactions and a large number of intermediates (CO₂, H₂O, CO, H₂, CH₄, toluene, etc.) in the process of biomass thermal conversion with in situ CO₂ capture, which cannot be simply explained by experiments. Molecular simulation can be utilized to study the reaction mechanism of a whole system, since it can save large amounts of manpower, materials, and time. Density functional theory (DFT) [17] plays an important role in the study of molecular simulation and is very convenient in the investigation of the adsorption mechanism of gas molecules on catalysts' surfaces. In recent years, studies on adsorption simulation using the DFT method have mainly focused on the optimization of different adsorption configurations and on the theoretical analysis of the adsorption behaviors of adsorbent surfaces and molecules. Hong et al. [18] studied the adsorption of CO₂ on the surface of CaO (001) at different coverages, from 1/9 monolayer (ML) to 1 ML using DFT calculations. The most stable adsorption structures at different coverages were obtained by analyzing the results. Sun et al. [19] simulated the dissociative adsorption of methane (DAM) on the surface of CaO (001) doped with Li, Na, K, and Cu. The calculations showed that the dopant lowers the energy of oxygen vacancy formation, increases the energy of the DAM reaction, and lowers the activation energy of DAM. Although some studies on the adsorption of gas molecules on the CaO surface have been reported, there are few studies on the simulation of small gas molecule adsorption on CaO-based sorbents in a biomass catalytic pyrolysis system.

In this paper, the adsorption characteristics of CO₂ on the surface of CaO and 10 wt % Ni/CaO catalysts at different temperatures in a biomass catalytic pyrolysis system were studied by DFT simulation and experimental methods. Hence the feasibility of DFT method was verified. Based on this premise, the adsorption behaviors of other molecules (CO, H₂O, H₂, and CH₄) on CaO and 10 wt % Ni/CaO (100) surfaces were further simulated to provide theoretical support for an in-depth analysis of complex catalytic reactions in biomass pyrolysis with in situ CO₂ capture and production of high-quality gas.

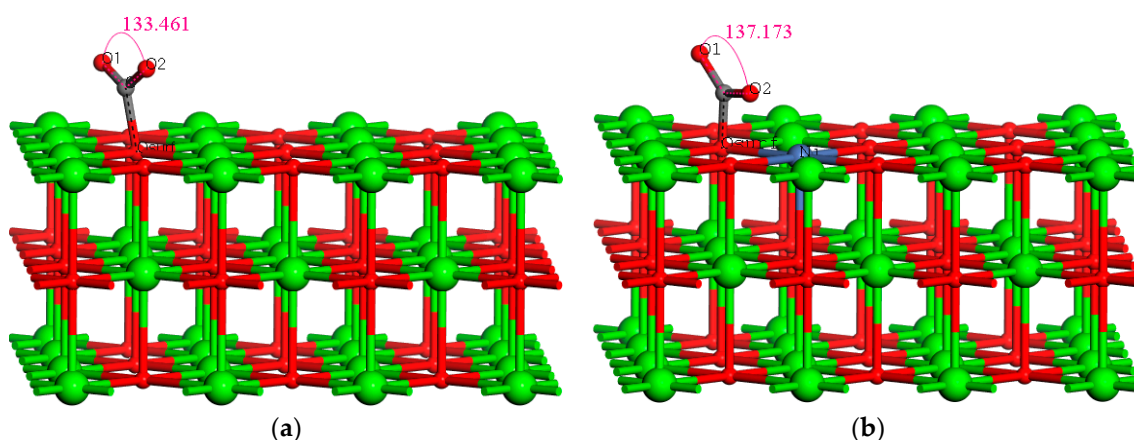
2. Results and Discussion

2.1. Comparison of Adsorption Characteristics of CO₂ on Two Catalyst Surfaces at Different Temperatures

The process of CO₂ adsorption on CaO and 10 wt % Ni/CaO (100) surfaces, at temperatures of 550, 600, 650, and 700 °C, was simulated by the DFT method. Table 1 shows the adsorption energies and geometrical parameters of CO₂ adsorbed on catalysts' surfaces. In the initial configuration of CO₂, the bond angle of O₁–C–O₂ was 180°, which changed after adsorption on the surface. Table 1 shows that CO₂ could be stably chemisorbed on the surface of the two catalysts. Moreover, the adsorption energy of CO₂ on the 10 wt % Ni/CaO (100) surface was significantly higher than on the CaO (100) surface, which proves that CO₂ is more likely to form a stable adsorption structure on the 10 wt % Ni/CaO (100) surface. Ni-doped CaO is conducive to enhancing the adsorption of CO₂ molecules on its surface, which promotes the in situ CO₂ capture in the reaction system. In the temperature range of 550–700 °C, the adsorption energies of CO₂ on CaO and 10 wt % Ni/CaO (100) surfaces increased and then weakened, reaching the maximum at 650 °C with 1.45 eV and 1.81 eV. The adsorption configurations of a single CO₂ molecule adsorbed on CaO and 10 wt % Ni/CaO (100) surfaces at 650 °C are presented in Figure 1, which shows that the C–O_{surf} bond lengths were 1.487 and 0.1343 nm, while the bond angles of O₁–C–O₂ were 133.461° and 137.173°, respectively.

Table 1. Geometrical parameters and adsorption energies of CO₂ on catalysts' surfaces at different temperatures.

	Temperature (°C)	Bond Length (Å)	Bond Angle (°)	E_{ads} (eV)
		C–O _{surf}	O ₁ –C–O ₂	
CaO	550	1.529	121.924	1.39
	600	1.517	127.350	1.41
	650	1.487	133.461	1.45
	700	1.493	138.341	1.43
10 wt % Ni/CaO	550	1.392	132.604	1.69
	600	1.373	136.249	1.74
	650	1.343	137.173	1.81
	700	1.357	127.228	1.77

**Figure 1.** Adsorption configurations of CO₂ on the surfaces of CaO-based catalysts at 650 °C: (a) CO₂ adsorption on CaO (100) surface; (b) CO₂ adsorption on 10 wt % Ni/CaO (100) surface. Green, red, gray, and purple balls represent Ca, O, C, and Ni atoms.

The density of states (DOS) can be used to characterize the electronic structure of a material. Figure 2 shows the partial density of states (PDOS) spectra of the O_{surf} atom at 650 °C. It should be noted from Figure 2a,b, which illustrates the PDOS of the O_{surf} atom on CaO and 10 wt % Ni/CaO (100) surfaces, that there were O_{surf} 2s and 2p peaks in the regions between −12 and −17 eV and 0 and −5 eV, respectively. Compared with the intensity of the O_{surf} 2p peak on the CaO (100) surface, the 10 wt % Ni/CaO surface decreased significantly, which can be explained by the Ni-doping affecting the electronic band structure of the O_{surf} atom, resulting in a decrease of the gravitational force between the nucleus and the outer electrons. It is clear from Figure 2c,d, which illustrates the PDOS of the O_{surf} atom on CaO-based catalyst surfaces after CO₂ adsorption, that the O_{surf} 2p peak split and moved to lower energy levels, indicating that the O_{surf} 2p orbital electrons participated in the bonding and transferred to the C atom. Similarly, the O_{surf} 2s peak also changed, which reveals that the O_{surf} 2s and the O_{surf} 2p orbitals both contributed to the C–O_{surf} chemical bond. The above results are taken as a proof that the CaO catalyst doped with Ni changes the electronic structure of the O_{surf} atom and is beneficial for strengthening the adsorption of CO₂ on the surface.

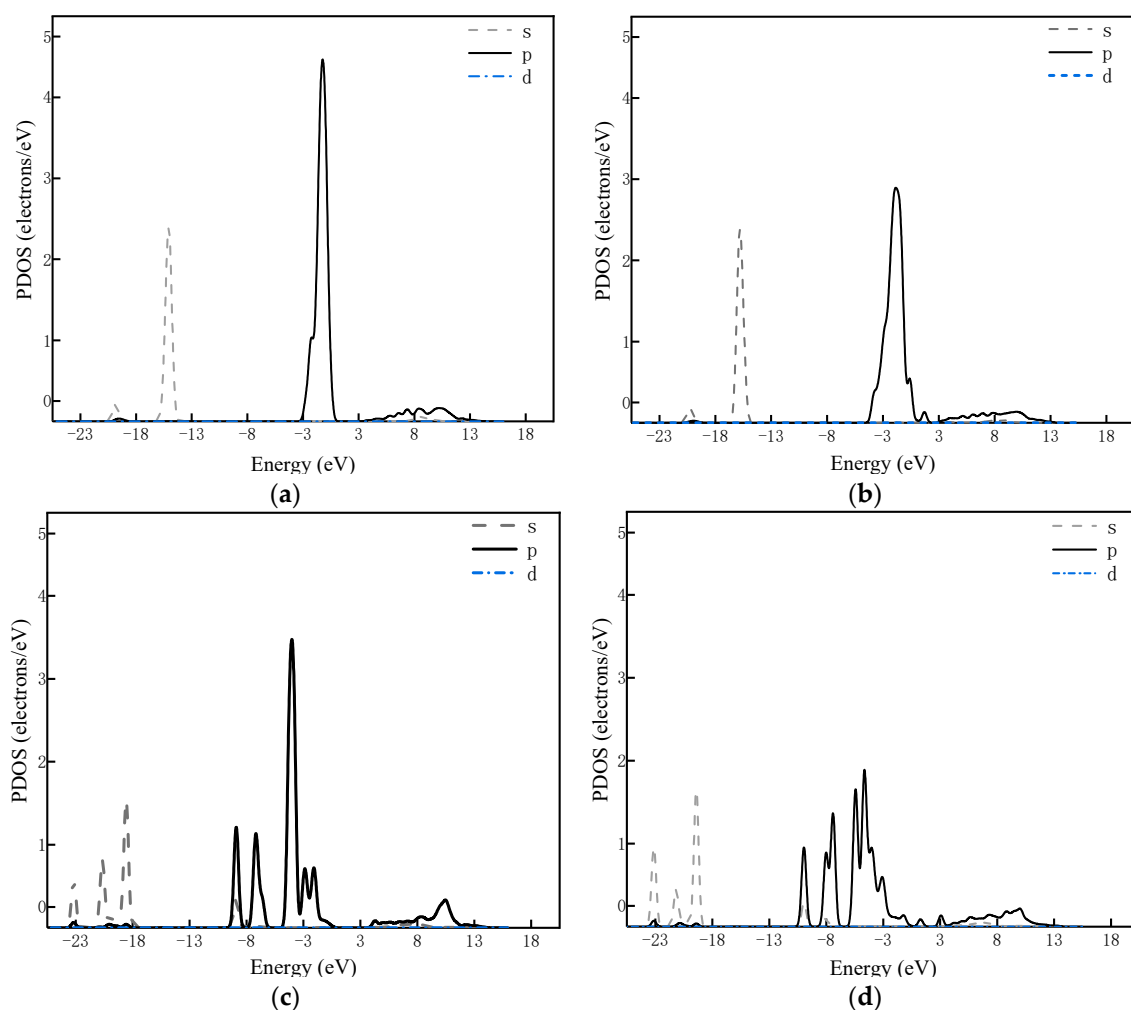


Figure 2. Partial density of states (PDOS) spectra of O_{surf} atoms: (a) the PDOS of the O_{surf} atom on CaO (100) surface; (b) the PDOS of the O_{surf} atom on 10 wt % Ni/CaO (100) surface; (c) the PDOS of the O_{surf} atom on CaO (100) surface after CO_2 adsorption; (d) the PDOS of the O_{surf} atom on 10 wt % Ni/CaO (100) surface after CO_2 adsorption.

Mulliken's population analysis reveals the strength of the chemical bond between atoms. The stability of the bonds decreases in a smaller bond population, while the possibility of the bond breaking increases during chemical reactions. Table 2 shows the bond populations of a CO_2 molecule before and after adsorption on the catalysts' surfaces. After adsorption, the Mulliken orbital population of C– O_1 and C– O_2 covalent bonds decreased. The bond population of CO_2 on the 10 wt % Ni/CaO (100) surface was smaller than on the CaO (100) surface, especially the population of the C– O_2 bond near the Ni atom, which reduced from 1.15 to 0.84. This indicates that Ni-doping decreases C–O bond stability in favor of the chemisorption reaction. This result provides strong evidence that CaO-based catalysts are beneficial to in situ CO_2 capture in biomass catalytic pyrolysis systems, and the decarbonization capability of the 10 wt % Ni/CaO catalyst is better than that of the CaO catalyst.

Table 2. Bond populations of CO_2 .

Orbital Population	CO_2	CO_2 on CaO (100)	CO_2 on 10 wt % Ni/CaO (100)
C– O_1	1.15	0.97	0.92
C– O_2	1.15	0.97	0.84

2.2. Analysis of CO₂ Temperature-Programmed Desorption (CO₂-TPD) Experimental Results at Different Temperatures

The CO₂-TPD experimental results are shown in Figure 3. At the adsorption temperatures of 550 °C, 600 °C, 650 °C, and 700 °C, both CaO and 10 wt % Ni/CaO catalysts presented a temperature-programmed desorption (TPD) peak. Figure 3 shows that when the adsorption temperatures increased, the intensity of the peaks rose and then decreased, reaching the highest values at 650 °C. The experimental results showed that the CO₂ adsorption capacities of the CaO-based catalysts were enhanced in the following order: 550 °C < 600 °C < 700 °C < 650 °C, in agreement with the trend of adsorption energies in the above DFT simulation. It can be concluded that the DFT simulation method is feasible to study the adsorption mechanism of other molecules on the catalysts' surfaces, which is beneficial for better understanding the complex catalytic reactions in biomass in situ CO₂ capture pyrolysis systems.

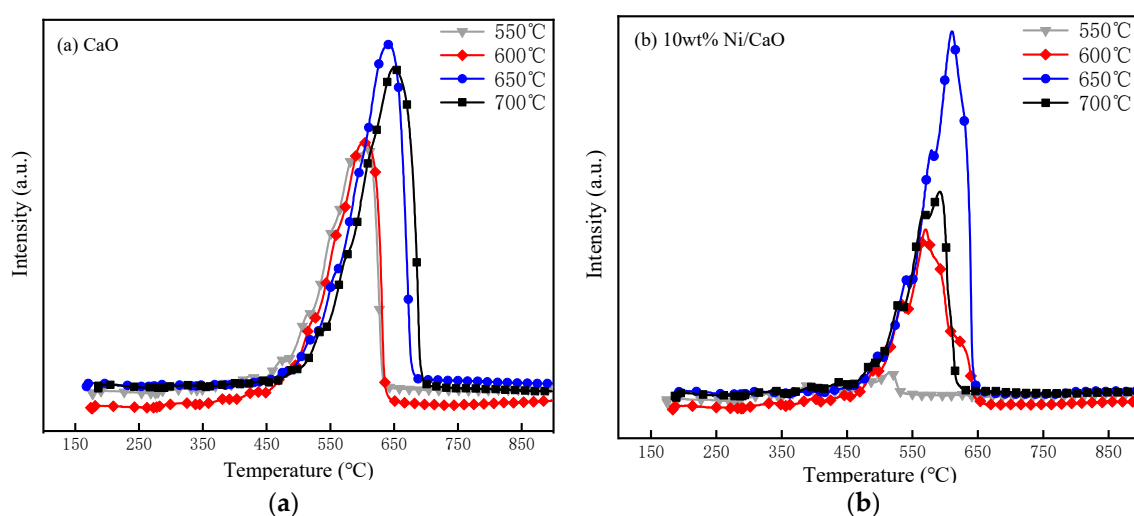


Figure 3. CO₂-TPD results of the examined catalysts: (a) the CO₂-TPD results of the CaO catalysts; (b) the CO₂-TPD results of the CaO catalysts.

2.3. Adsorption of H₂O, CO, H₂, and CH₄ on Catalysts' Surfaces

The above studies show that 650 °C is the most suitable temperature in the range of 550 °C–700 °C for the adsorption of CO₂ on the catalyst surface, which is conducive to the decarburizing reaction. Therefore, the adsorption energies of H₂O, CO, H₂, and CH₄ on CaO and 10 wt % Ni/CaO (100) surfaces at 650 °C were also calculated using the DFT method. By comparing the calculated adsorption energies, the adsorption competition mechanism of gas molecules on the catalyst surface was preliminarily identified.

Figure 4 shows the adsorption configurations of H₂O, CO, H₂, and CH₄ on CaO and 10 wt % Ni/CaO (100) surfaces at 650 °C. After adsorption on the CaO (100) surface, the adsorption energies were 2.05 eV, 0.351 eV, 0.136 eV, and 0.199 eV, respectively. Additionally, the adsorption energies of H₂O and CO molecules on the 10 wt % Ni/CaO (100) surface increased to 2.23 eV and 0.461 eV, respectively. The interaction between H₂O and the 10 wt % Ni/CaO (100) surface was relatively strong, indicating obvious chemical adsorption. However, the weak adsorption energies of H₂ and CH₄ on the surface were 0.162 eV and 0.183 eV, respectively, indicating that the adsorption should not be viewed as traditional chemisorption.

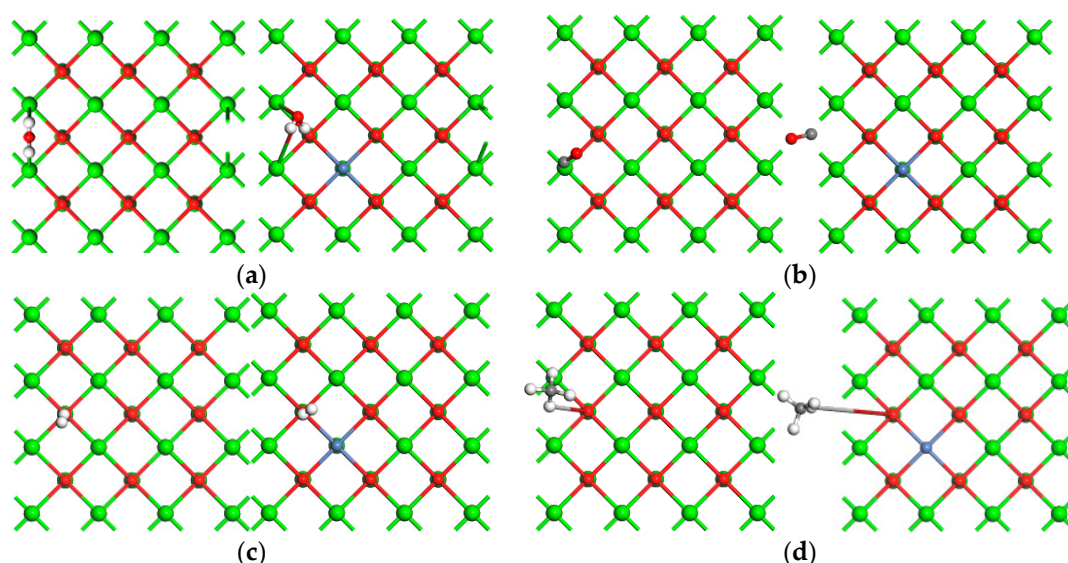


Figure 4. The adsorption configurations of gas molecules on CaO-based surfaces at 650 °C, left and right represent CaO and Ni/CaO: (a) the adsorption configuration of H₂O; (b) the adsorption configuration of CO; (c) the adsorption configuration of H₂; (d) the adsorption configuration of CH₄. Green, red, gray, white, and purple balls represent Ca, O, C, H, and Ni atoms.

The molecular competition mechanism on CaO-based catalyst surfaces was identified by DFT simulation. Table 3 shows the adsorption energies, which decreased in the following order: H₂O > CO₂ > CO > CH₄ > H₂. Among the molecules, the adsorption energy of H₂O was the largest, resulting in a preferential reaction which competed with the adsorption of CO₂ on the catalyst surface. The adsorption energies of CO, CH₄, and H₂ were so small that their effect on CO₂ adsorption was not worth considering. The increase of CO₂ adsorption energy on the 10 wt % Ni/CaO surface, in contrast with the CaO surface, was the largest, with the value increasing from 1.45 eV to 1.81 eV. Ni-doping obviously improved CO₂ adsorption capability of CaO; therefore, the 10 wt % Ni/CaO catalyst is conducive to in situ CO₂ capture in biomass pyrolysis. The adsorption capacity of each gas molecule on the catalyst surface affected the progress of each catalytic reaction in the system, so the molecular competition mechanism on the Ca-based catalyst provides a basis for adjusting the gas composition and preparing gas products directionally.

Table 3. Adsorption energies of gas molecules on 10 wt % Ni/CaO (100) surfaces.

<i>E</i> _{ads} (eV)	CO ₂	H ₂ O	CO	H ₂	CH ₄
CaO	1.45	2.05	0.361	0.136	0.199
10 wt % Ni/CaO	1.81	2.23	0.461	0.162	0.183

3. Computational and Experimental Methods

3.1. Computational Details

The first-principles calculations based on DFT were performed using the Cambridge Sequential Total Energy Package (CASTEP) and the Perdew-Wang-91 (PW91) functional within the generalized gradient approximation (GGA) [20]. The energy cutoff was set to 400 eV, and a $2 \times 2 \times 1$ *k*-point grid sampling was used for Brillouin-zone integration throughout the study [21–24]. The dynamics were calculated using the NVT ensemble, and the time step for the solution of dynamic KS equation was configured at 1.0 fs. The total simulate time was 1.5 ps, and the total number of steps was 1500 [25–27].

CaO has the same crystal structure as sodium chloride with a lattice parameter of 4.8105 nm, the space group of 225, Fm3m. In this study, the CaO (100) surface was selected for the investigation of the

adsorption behavior because it is the most stable surface of the CaO crystal [28]. Supercells (3×3) of the slab configurations, with a thickness of three layers, were used to study the adsorption properties of a CO₂ molecule, where only the adsorbate could relax. The thickness of the vacuum layer between the two adjacent layer planes was 1.5 nm, ensuring that the interaction force between the planes was small enough [29]. The adsorption energy (E_{ads}) is defined as:

$$E_{ads} = E_{adsorbate} + E_{surface} - E_{adsorption+system} \quad (1)$$

where $E_{adsorbate}$, $E_{surface}$, and $E_{adsorbate + surface}$ represent the energy of the catalyst surface, a gas molecule, and the total energy after adsorbing a gas molecule, respectively. If the adsorption energy obtained by simulation is within the range of 40–800 kJ/mol the process is chemical adsorption with strong adsorption. Otherwise, it is physical adsorption with relatively weak adsorption.

3.2. Experimental Details

CO₂ temperature-programmed desorption (CO₂-TPD) experiments were conducted using the chemical adsorption instrument FINESORB-3010 (Fantai, Hangzhou, Zhejiang, China). The samples were CaO catalyst prepared by calcining at 900 °C for 4 h, and 10 wt % Ni/CaO composite catalyst prepared by the method described in our previous study [5]. The samples were treated in high-purity carbon dioxide CO₂ ($\geq 99.999\%$) flow (15 mL/min) at 550, 600, 650, and 700 °C for 30 min. After that, they were cooled down to 100 °C in pure argon (Ar) ($\geq 99.999\%$) flow (20 mL/min) and then heated from 100 °C to 900 °C at a heating rate of 10 °C /min, while the TPD spectra was recorded continuously [30].

4. Conclusions

In this paper, the adsorption of CO₂ on Ca-based catalyst surfaces at different temperatures (550, 600, 650, and 700 °C) in the catalytic biomass pyrolysis system was studied using the DFT method and CO₂-TPD experiments. The results indicated that the adsorption capability of CO₂ on catalysts' surfaces was strongest at 650 °C. In addition, the adsorption competition mechanism of gas molecules was investigated using the DFT method, proving that, in contrast with a CaO surface, a 10 wt % Ni/CaO surface is conducive to in situ CO₂ capture in biomass pyrolysis. The above results provide theoretical support for in-depth studies on complex catalytic reactions in biomass pyrolysis with in situ CO₂ capture.

Author Contributions: Conceptualization, H.G.; Formal analysis, J.W.; Funding acquisition, B.Z. and D.Z.; Investigation, J.W., G.S., and H.Y.; Methodology, J.W., L.S., and S.Y.; Project administration, B.Z.; Resources, L. C. and X.X.; Supervision, B.Z.; Validation, B.Z.; Writing—original draft, J.W.; Writing—review & editing, B.Z.

Funding: This work was supported by National Key R&D Program of China (2018YFE0106400), Shandong Provincial Key Research and Development Plan (2018GGX104028 and 2018GGX104026), Natural Science Foundation of Shandong Province of China (ZR2019MEE069, ZR2019MB061, ZR2016YL010 and ZR2016YL012).

Acknowledgments: The authors would like to thank all the laboratory technicians.

Conflicts of Interest: There are no conflicts to declare.

References

1. Zhao, B.; Zhang, X.; Xu, A.; Ding, W.; Sun, L.; Chen, L.; Guan, H.; Yang, S.; Zhou, W. A study of the in-situ CO₂ removal pyrolysis of Chinese herb residue for syngas production. *Sci. Total Environ.* **2018**, *626*, 703–709. [CrossRef] [PubMed]
2. Xu, A.; Zhou, W.; Zhang, X.; Zhao, B.; Chen, L.; Sun, L.; Ding, W.; Yang, S.; Guan, H.; Bai, B. Gas production by catalytic pyrolysis of herb residues using Ni/CaO catalysts. *J. Anal. Appl. Pyrolysis* **2018**, *130*, 216–223. [CrossRef]
3. Zhao, B.; Zhang, X.; Chen, L.; Sun, L.; Si, H.; Chen, G. High quality fuel gas from biomass pyrolysis with calcium oxide. *Bioresour. Technol.* **2014**, *156*, 78–83. [CrossRef] [PubMed]

4. Charisiou, N.D.; Baklavaridis, A.; Papadakis, V.G.; Goula, M.A. Synthesis Gas Production via the Biogas Reforming Reaction Over Ni/MgO–Al₂O₃ and Ni/CaO–Al₂O₃ Catalysts. *Waste Biomass Valorization* **2016**, *7*, 725–736. [\[CrossRef\]](#)
5. Bennici, S.; Jeguirim, M.; Limousy, L.; Haddad, K.; Vaulot, C.; Michelin, L.; Josien, L.; Zorpas, A.A. Influence of CO₂ Concentration and Inorganic Species on the Gasification of Lignocellulosic Biomass Derived Chars. *Waste Biomass Valorization* **2019**, 1–8. [\[CrossRef\]](#)
6. Wang, M.; Qi, Y.; Ma, R.; Fu, Z.; Ge, P.; Ji, S.; Wu, J.; Qian, X. Investigation of CaO Influences on Fst Gasification Characteristics of Biomass in a Fixed-bed Reactor. *Waste Biomass Valorization* **2019**, 1–8.
7. Li, J.; Wang, H.; Zhu, Q.; Li, H. Coupling relationship of fluidization behavior, reaction and particle structure of Ni/MgO catalyst toward fluidized CO methanation. *Chem. Eng. J.* **2019**, *357*, 298–308. [\[CrossRef\]](#)
8. Yang, H.; Wang, D.; Li, B.; Zeng, Z.; Qu, L.; Zhang, W.; Chen, H. Effects of potassium salts loading on calcium oxide on the hydrogen production from pyrolysis-gasification of biomass. *Bioresour. Technol.* **2017**, *249*, 744–750. [\[CrossRef\]](#)
9. Khan, Z.; Yusup, S.; Ahmad, M.M. Performance Study of Ni Catalyst with Quicklime (CaO) as CO₂ Adsorbent in Palm Kernel Shell Steam Gasification for Hydrogen Production. *Adv. Mater. Res.* **2014**, *917*, 283–291. [\[CrossRef\]](#)
10. Jiang, S.; Lu, Y.; Wang, S.; Zhao, Y.; Ma, X. Insight into the reaction mechanism of CO₂ activation for CH₄ reforming over NiO–MgO: A combination of DRIFTS and DFT study. *Appl. Surf. Sci.* **2017**, *416*, 59–68. [\[CrossRef\]](#)
11. Naeem, M.A.; Armutlulu, A.; Imtiaz, Q.; Müller, C.R. CaO-Based CO₂ Sorbents Effectively Stabilized by Metal Oxides. *Chemphyschem* **2017**, *18*, 3280–3285. [\[CrossRef\]](#) [\[PubMed\]](#)
12. Charisiou, N.D.; Papageridis, K.N.; Tzounis, L.; Sebastian, V.; Hinder, S.J.; Baker, M.A.; AlKetbi, M.; Polychronopoulou, K.; Goula, M.A. Ni supported on CaO–MgO–Al₂O₃ as a highly selective and stable catalyst for H₂ production via the glycerol steam reforming reaction. *Int. J. Hydrog. Energy* **2018**, *8*, 256–273. [\[CrossRef\]](#)
13. Tao, J.; Zhao, L.; Dong, C.; Lu, Q.; Du, X.; Dahlquist, E. Catalytic Steam Reforming of Toluene as a Model Compound of Biomass Gasification Tar Using Ni–CeO₂/SBA-15 Catalysts. *Energies* **2013**, *6*, 3284–3296. [\[CrossRef\]](#)
14. Li, B.; Yang, H.; Wei, L.; Shao, J.; Wang, X.; Chen, H. Absorption-enhanced steam gasification of biomass for hydrogen production: Effects of calcium-based absorbents and NiO-based catalysts on corn stalk pyrolysis-gasification. *Int. J. Hydrog. Energy* **2017**, *42*, 5840–5848. [\[CrossRef\]](#)
15. Radfarnia, H.R.; Iliuta, M.C. Development of Al-stabilized CaO–nickel hybrid sorbent–catalyst for sorption-enhanced steam methane reforming. *Chem. Eng. Sci.* **2014**, *109*, 212–219. [\[CrossRef\]](#)
16. Wei, L.; Xu, S.; Liu, J.; Liu, C.; Liu, S. Hydrogen Production in Steam Gasification of Biomass with CaO as a CO₂ Absorbent. *Energy Fuels* **2008**, *22*, 1997–2004. [\[CrossRef\]](#)
17. Vanderbilt, D. Soft self-consistent pseudopotentials in a generalized eigenvalue formalism. *Phys. Rev. B Condens. Matter* **1990**, *41*, 7892. [\[CrossRef\]](#)
18. Chen, H.; Zhang, Y.; Li, Y.; Huang, S.; Qi, J.; Liu, R. A DFT Study on the Adsorption of CO₂ Molecules on CaO(001) Surface at Different Coverages. *Chin. J. Struct. Chem.* **2019**, *38*, 17–24.
19. Sun, X.; Li, B.; Metiu, H. Methane Dissociation on Li-, Na-, K-, and Cu-Doped Flat and Stepped CaO(001). *J. Phys. Chem. C* **2013**, *117*, 7114–7122. [\[CrossRef\]](#)
20. Perdew, J.P.; Chevary, J.A.; Vosko, S.H.; Jackson, K.A.; Pederson, M.R.; Singh, D.J.; Fiolhais, C. Atoms, molecules, solids, and surfaces: Applications of the generalized gradient approximation for exchange and correlation. *Phys. Rev. B Condens. Matter* **1993**, *46*, 6671–6687. [\[CrossRef\]](#)
21. Zhao, L.; Wu, Y.; Han, J.; Lu, Q.; Yang, Y.; Zhang, L. Mechanism of Mercury Adsorption and Oxidation by Oxygen over the CeO₂(111) Surface: A DFT Study. *Materials* **2018**, *11*, 485. [\[CrossRef\]](#) [\[PubMed\]](#)
22. Wei, H.; Gui, Y.; Kang, J.; Wang, W.; Tang, C. A DFT Study on the Adsorption of H₂S and SO₂ on Ni Doped MoS₂ Monolayer. *Nanomaterials* **2018**, *8*, 646. [\[CrossRef\]](#) [\[PubMed\]](#)
23. Fan, Y.; Zhuo, Y.; Lou, Y.; Zhu, Z.; Li, L. SeO₂ adsorption on CaO surface: DFT study on the adsorption of a single SeO₂ molecule. *Appl. Surf. Sci.* **2017**, *413*, 366–371. [\[CrossRef\]](#)
24. Pan, Y.X.; Liu, C.J.; Ge, Q. Effect of surface hydroxyls on selective CO₂ hydrogenation over Ni₄/γ-Al₂O₃: A density functional theory study. *J. Catal.* **2010**, *272*, 227–234. [\[CrossRef\]](#)

25. Besson, R.; Vargas, M.R.; Favregeon, L. CO₂ adsorption on calcium oxide: An atomic-scale simulation study. *Surf. Sci.* **2012**, *606*, 490–495. [[CrossRef](#)]
26. Yang, C. DFT Study of the Effect of Temperature on ZnO Adsorbed on α -Al₂O₃(0001) Surface. *Chin. J. Chem. Phys.* **2006**, *19*, 137–142. [[CrossRef](#)]
27. Liang, X.Q.; Qiu, L.F.; Huang, P.; Yang, C. A DFT Study of TiO₂ Adsorption on GaN(0001) Line Defect Surface. *Adv. Mater. Res.* **2013**, *807*, 2836–2841. [[CrossRef](#)]
28. Li, X.; An, M.; Zhu, Y.; Ma, H. First-Principles Study Adsorption Properties Of CO₂ Molecule on CaO(100) Surfaces. In Proceedings of the 2nd International Workshop on Materials Engineering and Computer Sciences, Jinan, China, 10–11 October 2015; Volume 33, pp. 267–270.
29. Wang, W.; Fan, L.; Wang, G.; Li, Y. CO₂ and SO₂ sorption on the alkali metals doped CaO(100) surface: A DFT-D study. *Appl. Surf. Sci.* **2017**, *425*, 972–977. [[CrossRef](#)]
30. Yang, S.; Zhang, X.; Lei, C.; Sun, L.; Xie, X.; Zhao, B. Production of syngas from pyrolysis of biomass using Fe/CaO catalysts: Effect of operating conditions on the process. *J. Anal. Appl. Pyrolysis* **2017**, *125*, 1–8. [[CrossRef](#)]



© 2019 by the authors. Licensee MDPI, Basel, Switzerland. This article is an open access article distributed under the terms and conditions of the Creative Commons Attribution (CC BY) license (<http://creativecommons.org/licenses/by/4.0/>).